VSPIN: a new model relying on the vectorial description of the laser field for predicting the polarization dynamics of spin-injected V(e)CSELs

Mehdi Alouini, Julien Frougier, Alexandre Joly, Ghaya Baili, Daniel Dolfi, Jean-Marie George

Research Article | Vol. 26, No. 6 | 19 Mar 2018 | OPTICS EXPRESS 6739
Optics EXPRESS

VSPIN: a new model relying on the vectorial description of the laser field for predicting the polarization dynamics of spin-injected V(e)CSELs

MEHDI ALOUINI,[1,2,*] JULIEN FROUGIER,[3] ALEXANDRE JOLY,[1,2] GHAYA BAILI,[2] DANIEL DOLFI,[2] AND JEAN-MARIE GEORGE[3]

[1]*Institut Foton, Université de Rennes 1, CNRS, Campus de Beaulieu, 35042 Rennes, France*
[2]*Thales Research & Technology, 1 av. Augustin Fresnel, 91767 Palaiseau Cedex, France*
[3]*Unité Mixte de Physique CNRS-Thales, 1 av. Augustin Fresnel, 91767 Palaiseau, France*
**mehdi.alouini@univ-rennes1.fr*

Abstract: A new vectorial model (VSPIN) based on the Jones formalism is proposed to describe the polarization dynamics of spin injected V(e)CSELs. This general modelling framework accounts for spin injection effects as a gain circular dichroism in the active medium and provides guidelines for developing functional spin-controlled lasers. We investigate the detrimental role of phase anisotropy on polarization switching and show that it can be overcome by preparing the laser cavity to achieve efficient polarization switching under low effective spin injection. The VSPIN model predictions have been confirmed experimentally and explain the polarization behavior of spin-VCSELs reported in the literature.

OCIS codes: (140.7260) Vertical cavity surface emitting lasers; (140.3430) Laser theory; (140.3410) Laser resonators; (260.5430) Polarization; (200.6715) Switching.

References and links

1. R. Fiederling, M. Keim, G. Reuscher, W. Ossau, G. Schmidt, A. Waag, and L. W. Molenkamp, "Injection and detection of a spin-polarized current in a light-emitting diode," Nature **402**(6763), 787–790 (1999).
2. X. Jiang, R. Wang, R. M. Shelby, R. M. Macfarlane, S. R. Bank, J. S. Harris, and S. S. P. Parkin, "Highly Spin-Polarized Room-Temperature Tunnel Injector for Semiconductor Spintronics using MgO(100)," Phys. Rev. Lett. **94**(5), 056601 (2005).
3. S. A. Crooker, D. D. Awschalom, J. J. Baumberg, F. Flack, and N. Samarth, "Optical spin resonance and transverse spin relaxation in magnetic semiconductor quantum wells," Phys. Rev. B **56**(12), 7574–7588 (1997).
4. A. Garnache, A. Ouvrard, and D. Romanini, "Single-Frequency operation of External-Cavity VCSELs: Non-linear multimode temporal dynamics and quantum limit," Opt. Express **15**(15), 9403–9417 (2007).
5. J. Lee, W. Falls, R. Oszwaldowski, and I. Zutic, "Spin modulation in semiconductor lasers," Appl. Phys. Lett. **97**(4), 041116 (2010).
6. N. Gerhardt, S. Hovel, M. Hofmann, J. Yang, D. Reuter, and A. Wieck, "Enhancement of spin information with vertical cavity surface emitting lasers," Electron. Lett. **42**(2), 88–89 (2006).
7. P. E. Faria, G. Xu, G. Lee, N. C. Gerhardt, G. M. Sipahi, and I. Zutic, "Toward high-frequency operation of spin lasers," Phys. Rev. B **92**(7), 075311 (2015).
8. D. Basu, D. Saha, and P. Bhattacharya, "Optical polarization modulation and gain anisotropy in an electrically injected spin laser," Phys. Rev. Lett. **102**(9), 093904 (2009).
9. S. Hovel, N. Gerhardt, M. Hofmann, J. Yang, D. Reuter, and A. Wieck, "Spin controlled optically pumped vertical cavity surface emitting laser," Electron. Lett. **41**(5), 251–253 (2005).
10. M. Holub, J. Shin, S. Chakrabarti, and P. Bhattacharya, "Electrically injected spin-polarized vertical-cavity surface-emitting lasers," Appl. Phys. Lett. **87**(9), 091108 (2005).
11. J. Rudolph, S. Döhrmann, D. Hägele, M. Oestreich, and W. Stolz, "Room-temperature threshold reduction in vertical-cavity surface-emitting lasers by injection of spin-polarized electrons," Phys. Rev. Lett. **87**(24), 241117 (2005).
12. J. Lee, S. Bearden, E. Wasner, and I. Žutić, "Spin-lasers: From threshold reduction to large-signal analysis," Appl. Phys. Lett. **105**(4), 042411 (2014).
13. E. Wasner, S. Bearden, J. Lee, and I. Žutić, "Digital operation and eye diagrams in spin-lasers," Appl. Phys. Lett. **107**(8), 082406 (2015).

#318099 https://doi.org/10.1364/OE.26.006739
Journal © 2018 Received 20 Dec 2017; revised 3 Feb 2018; accepted 15 Feb 2018; published 6 Mar 2018

Optics EXPRESS

14. H. Ando, T. Sogawa, and H. Gotoh, "Photon-spin controlled lasing oscillation in surface-emitting lasers," Appl. Phys. Lett. **73**(5), 566–568 (1998).
15. M. Travagnin, J. P. Woerdman, A. K. Jansen van Doorn, J. P. Woerdman, "Role of optical anisotropies in the polarization properties of surface-emitting semiconductor lasers," Phys. Rev. A **54**(2), 1647–1660 (1996).
16. M. Travagnin, M. P. van Exter, A. K. Jansen van Doorn, and J. P. Woerdman, "Erratum: Role of optical anisotropies in the polarization properties of surface emitting semiconductor lasers [phys. rev. a 54, 1647 (1996)]," Phys. Rev. A **55**(6), 4641 (1997).
17. J. Frougier, G. Baili, I. Sagnes, D. Dolfi, J.-M. George, and M. Alouini, "Accurate measurement of the residual birefringence in VECSEL: Towards understanding of the polarization behavior under spin-polarized pumping," Opt. Express **23**(8), 9573–9588 (2015).
18. Q. Feng, J. V. Moloney, and J. V. Moloney,"Light-polarization dynamics in surface-emitting semiconductor lasers," Phys. Rev. A **52**(2), 1728–1739 (1995).
19. A. Gahl, S. Balle, and M. S. Miguel, "Polarization dynamics of optically pumped vcsels," IEEE J. Quantum Electron. **35**(3), 342–351 (1999).
20. C. Gøthgen, R. Oszwałdowski, A. Petrou, and I. Žutić, "Analytical model of spin-polarized semiconductor lasers," Appl. **93**(4), 042513 (2008).
21. S. De, V. Potapchuk, and F. Bretenaker, "Influence of spin-dependent carrier dynamics on the properties of a dual-frequency vertical-external-cavity surface-emitting laser," Phys. Rev. A **90**(1), 013841 (2014).
22. J. Frougier, G. Baili, M. Alouini, I. Sagnes, H. Jaffrès, A. Garnache, C. Deranlot, D. Dolfi, and J. M. George, "Control of light polarization using optically spin-injected vertical external cavity surface emitting lasers," Appl. Phys. Lett. **103**(25), 252402 (2013).
23. A. Joly, G. Baili, M. Alouini, J.-M. George, I. Sagnes, G. Pillet, and D. Dolfi, "Compensation of the residual linear anisotropy of phase in a vertical-external-cavity-surface-emitting laser for spin injection," Opt. Lett. **42**(3), 651–654 (2017).
24. R. C. Jones, "A new calculus for the treatment of optical systems. I. Description and discussion of the calculus," J. Opt. Soc. Am. **31**(7), 488–493 (1941).
25. A. E. Siegman, *Lasers* (University Science Books, 1986).
26. A. Le Floch, G. Ropars, J. M. Lenormand, and R. Le Naour, "Dynamics of Laser Eigenstates," Phys. Rev. Lett. **52**(11), 918–921 (1984).
27. E. Collett, *Polarized Light: Fundamentals and Applications* (Dekker, 1993).
28. C. Brosseau, *Fundamentals of Polarized Light: A Statistical Optics Approach* (Wiley, 1998).
29. S. Iba, S. Koh, K. Ikeda, and H. Kawaguchi, "Room temperature circularly polarized lasing in an optically spin injected vertical-cavity surface-emitting laser with (110) GaAs quantum wells," Appl. Phys. Lett. **98**(8), 081113 (2011).
30. T. Fördös, K. Postava, H. Jaffrès, and J. Pištora, "Matrix approach for modeling of emission from multilayer spin-polarized light-emitting diodes and lasers," J. Opt. **16**(6), 065008 (2014).
31. N. Ortega-Quijano, J. Fade, F. Parnet, and M. Alouini, "Generation of a coherent light beam with precise and fast dynamic control of the state and degree of polarization," Opt. Lett. **42**(15), 2898–2901 (2017).
32. N. C. Gerhardt, M. Y. Li, H. Jähme, H. Höpfner, T. Ackemann, and M. R. Hofmann, "Ultrafast spin-induced polarization oscillations with tunable lifetime in vertical-cavity surface-emitting lasers," Appl. Phys. Lett. **99**(15), 151107 (2011).
33. V. Pal, P. Trofimoff, B.-X. Miranda, G. Baili, M. Alouini, L. Morvan, D. Dolfi, F. Goldfarb, I. Sagnes, R. Ghosh, and F. Bretenaker, "Measurement of the coupling constant in a two-frequency VECSEL," Opt. Express **18**(5), 5008–5014 (2010).
34. M. Vallet, M. Brunel, M. Alouini, F. Bretenaker, A. Le Floch, and G. P. Agrawal, "Polarization self-modulated lasers with circular eigenstates," Appl. Phys. Lett. **74**(22), 3266–3268 (1999).
35. M. B. Willemsen, J. P. Woerdman, and J. P. Woerdman, "Anatomy of a Polarization Switch of a Vertical-Cavity Semiconductor Laser," Phys. Rev. Lett. **84**(19), 4337–4340 (2000).
36. M. Sargent, III M. O. Scully, and W. E. Lamb, Jr., *Laser Physics* (Addison-Wesley, 1974).
37. M. Brunel, M. Vallet, A. Le Floch, and F. Bretenaker, "Differential measurement of the coupling constant between laser eigenstates," Appl. Phys. Lett. **70**(16), 2070–2072 (1997).
38. M. Alouini, F. Bretenaker, M. Brunel, A. Le Floch, M. Vallet, and P. Thony, "Existence of two coupling constants in microchip lasers," Opt. Lett. **25**(12), 896–898 (2000).
39. A. McKay, J. M. Dawes, and J. D. Park, "Polarisation-mode coupling in (100)-cut Nd:YAG," Opt. Express **15**(25), 16342–16347 (2007).
40. G. Baili, L. Morvan, M. Alouini, D. Dolfi, F. Bretenaker, I. Sagnes, and A. Garnache, "Experimental demonstration of a tunable dual-frequency semiconductor laser free of relaxation oscillations," Opt. Lett. **34**(21), 3421–3423 (2009).

1. Introduction

Spin-injection into semiconductor (SC) based Light Emitting Diodes (LED) is currently the subject of significant research effort [1,2]. In these devices, quantum selection rules associated with the angular momentum make it possible to convert electronic spin information into photon polarization information [3]. State of the art spin-LEDs are shown to

Optics EXPRESS

provide good conversion efficiency leading to a degree of circular polarization (DoCP) as high as 90% at 1.5 K and with a 3 T external magnetic field [1]. Spin-lasers are also expected to exhibit better performances in terms of DoCP due to the presence of an optical cavity imposing a resonant condition to the electro-magnetic field, including its polarization [4–7]. In comparison to SC edge-emitting lasers, where the polarization state is mainly defined by the optical waveguide, Vertical-Cavity Surface Emitting Lasers (VCSELs) appear to be good candidates for a spin-laser [8–11]. As compared to spin-unpolarized lasers, spin-lasers offer interesting properties such as improvement of modulation bandwidth, threshold reduction, new modulation format by coding the light polarization state, and better eye diagram [8,12,13]. Therefore, spin injected lasers, operating at RT without external magnetic field, could be one of the future technological breaking devices in the telecommunication domain. Nevertheless, it is shown that excessive residual linear anisotropies can fix the polarization eigenstates to linear polarizations [14–17], preventing any visible effect of spin injection especially when the spin coherence is barely maintained. Several models based on rate equations and including spin dependent carrier dynamics have already been developed for VCSELs in order to describe the evolution of the polarization eigenstates with different degrees of accuracy [18–21]. However, these models mainly consider carriers' dynamics in the active medium taking into account microscopic parameters or assume that the laser polarization state is similar to that provided by the gain structure. The use of an external laser cavity such as for Vertical external-Cavity Surface emitting Lasers (VeCSELs) enables the insertion of additional optical components inside the laser cavity to possibly reveal the effect of spin injection on the laser polarization. For instance, we have shown that preparing the laser cavity so that its two possible polarization eigenstates correspond to left and right circular polarizations is the optimal architecture for stimulating a full polarization switch even with very poor spin injection efficiency [22]. Nevertheless, the need for an intra-cavity Faraday rotator to compensate the residual anisotropy of the semiconductor structure makes this approach cumbersome and difficult to implement for a realistic marketable device. More recently, we have shown that compensating the linear phase anisotropy in the cavity is another way to stimulate polarization switching through spin injection, but is less efficient [23]. These experimental developments have been guided by a simple and pragmatic modelling approach taking into account the presence of additional optical components inside the laser cavity and considering that spin injection phenomenologically leads to a tiny gain circular dichroism in the active medium.

In this paper, we describe this model step by step and show how it can successfully predict the polarization behavior of the laser and how it sets general guidelines for implementing a laser sensitive to low efficiency spin injection. The Vectorial-SPIN (VSPIN) model presented in this work relies on the derivation of the field resonant condition in the framework of the Jones formalism.

2. Modelling spin lasers including residual phase anisotropy

The Jones formalism [24] offers an ideal framework for determining the polarization state of a laser. Indeed, in the steady state, the resonance condition imposed by the laser cavity makes the field coherent by definition leading to a well-defined state of polarization [25]. The determination of the laser characteristics, i.e. longitudinal and transverse distributions of the field as well as the associated gain and frequency, can thus be performed by solving the resonant condition for a 2×2 Jones matrix which takes into account all the elements inside the cavity including the active medium [26]. As in any laser, the cold cavity exhibits always a residual linear anisotropy of phase [15], which defines the two polarization eigenstates of the cavity. Note that linear phase anisotropy might be termed in the literature as "birefringence" or "linear birefringence". One assumes that this phase anisotropy comes from the active medium and can be represented by a thin birefringent layer, as sketched in Fig. 1. The associated Jones matrix is [27,28]

Optics EXPRESS

$$\left[J_{\Delta\phi}\right]=e^{-i\frac{2\pi}{\lambda_0}\bar{n}l}\begin{bmatrix}e^{-i\frac{\gamma}{2}} & 0\\ 0 & e^{i\frac{\gamma}{2}}\end{bmatrix}, \tag{1}$$

where γ denotes this phase anisotropy, λ_0 is the mean laser wavelength, and l is the optical length of the cavity. $\bar{n}=(n_e+n_o)/2$ is the mean refractive index of the birefringent element, where n_o and n_e are the ordinary and extraordinary indices of the birefringence, respectively. Accordingly, the phase anisotropy reads

$$\gamma=\frac{2\pi}{\lambda_0}(n_e-n_0)l. \tag{2}$$

Under these conditions, the cold cavity exhibits two eigenstates, which are linearly polarized along the ordinary and extraordinary axes of the residual birefringence. The next step is to determine to what extent a circular dichroism of gain, also termed in the literature as "gain anisotropy" or "gain asymmetry", induced by preferential spin injection can modify these eigenstates and lead to circularly polarized eigenstates, as already observed in the literature for spin lasers [29]. This dichroism can be either measured experimentally or predicted theoretically for a given active medium taking into account light/matter interaction within the actual multilayer structure [30]. We define the circular dichroism of gain for a total back and forth interaction of the field as $\Delta G=G_R-G_L$. The associated Jones matrix reads:

$$\left[J_{\Delta G}\right]=\begin{bmatrix}\bar{G} & -\frac{i}{2}\Delta G\\ \frac{i}{2}\Delta G & \bar{G}\end{bmatrix}. \tag{3}$$

In this matrix, $\bar{G}=(G_R-G_L)/2$ represents the active medium mean gain, where G_R et G_L are the gains seen by right hand and left hand circular polarized fields, respectively. The matrix $\left[J_{\Delta G}\right]$ does not bring any phase anisotropy, γ, as long as circular polarizations are considered, right or left handed. However, it induces a phase term when the incident polarization is linear leading to an elliptical output polarization, whose ellipticity increases with the gain circular dichroism. In other words, the gain circular dichroism ΔG induces the projection of a linear polarization field onto the orthogonal state.

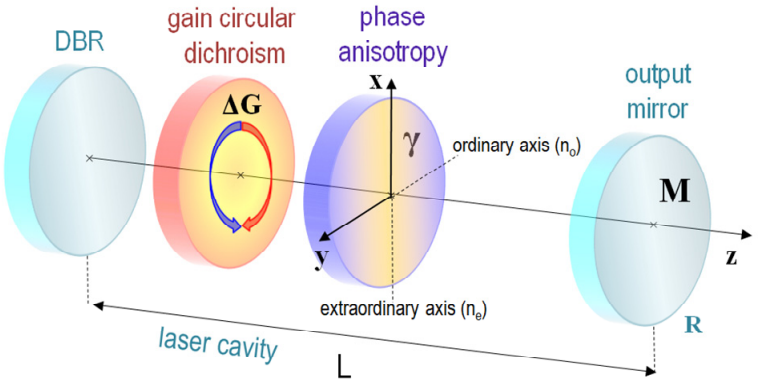

Fig. 1. Schematic representation of the cavity.

Optics EXPRESS

We now assume that the cavity input mirror is perfectly reflecting and isotropic such that its presence can be omitted in this vectorial formalism. Note that this hypothesis is not restrictive, since any residual birefringence in the mirror could be taken into account in the previously introduced Jones matrix modeling a birefringent element. Finally, assuming that the output coupler is isotropic and that its electric field reflectivity is R, the associated Jones matrix reads:

$$[J_M] = \sqrt{R}\begin{bmatrix} 1 & 0 \\ 0 & 1 \end{bmatrix}. \tag{4}$$

Let us now consider that the axes of the residual birefringence are oriented along x and y, z being the propagation axis (see Fig. 1). The total Jones matrix of the field at the output mirror after one round trip of the cavity is

$$[J_L] = e^{i\phi}\left[J_{\Delta\phi}\right][J_G]\left[J_{\Delta\phi}\right][J_M]. \tag{5}$$

In this expression, the Jones matrix $[J_G]$ associated to the gain takes into account the back and forth interaction of the field with the laser components while $e^{j\phi}$ is the cumulative phase after one roundtrip propagation through the cavity. Developing Eq. (5) yields

$$[J_L] = \sqrt{R}\,\bar{G}\,e^{-2ik(n_{ma}e_{ma}+\bar{n}l+L)}\begin{bmatrix} e^{-i\gamma} & -\frac{i}{2}\Delta G_N \\ \frac{i}{2}\Delta G_N & e^{i\gamma} \end{bmatrix}, \tag{6}$$

where $k = 2\pi\nu/c$ is the electromagnetic field wave number, n_{ma} and e_{ma} are the refractive index and the thickness of the active medium, and L is the cavity length excluding the active medium and the birefringent plate. In the case of a monolithic VCSEL, L = 0. Finally, $\Delta G_N = \Delta G/\bar{G}$ holds for the normalized circular dichroism of gain. For the sake of conciseness, we define the effective length, $L_{eff} = n_{ma}e_{ma} + \bar{n}l + L$, representing the mean optical length of the cavity.

The resonance condition of the field $\vec{E}$ for one round trip in the cavity imposes that

$$[J_L]\vec{E} = \lambda\vec{E}. \tag{7}$$

In this expression, λ are the eigenvalues. The system considered here having two degrees of freedom, two eigenvalues are possible. The diagonalization of the $[J_L]$ matrix enables to solve for the two complex eigenvalues. These contain both the frequency and gain of each mode, as well as the associated eigenvectors describing the two possible polarization states. The characteristic polynomial obtained by solving Eq. (7) is:

$$\left(\lambda - \cos(\gamma)\right)^2 = \frac{1}{4}\Delta G_N^2 - \sin^2(\gamma). \tag{8}$$

The laser behavior is ruled by this equation, so different oscillation regimes will appear depending on the relative ratio between the linear anisotropy of phase γ and the circular dichroism of the gain ΔG_N. Furthermore, the saturated gains and the laser oscillation frequencies in the eigenbasis are connected to the eigenvalues through

$$\lambda = \frac{1}{\sqrt{R}\,\bar{G}}\mathrm{e}^{-2ik\,L_{eff}}. \tag{9}$$

Optics EXPRESS

2.1 Study of specific cases

2.1.1 The circular dichroism of the gain is zero, $\Delta G_N = 0$ (no effective spin-polarization in the active medium)

When the circular dichroism of the gain is zero, the only contribution to the laser behavior comes from the residual linear birefringence γ. The Jones Matrix of the laser $[J_L]$ is already diagonal, so that the two eigenvectors correspond to two crossed linear polarizations oriented along the neutral axes of the birefringence, that is:

$$\frac{E_y}{E_x} = 0 \quad or \quad \frac{E_y}{E_x} \to \infty. \tag{10}$$

Moreover, Eq. (8) simplifies to $\left(\lambda - \cos(\gamma)\right)^2 = \cos^2(\gamma) - 1$ leading to $\lambda_\pm = e^{\pm i\gamma}$. Consequently, the frequency difference between the two eigenstates is equal to

$$\Delta\nu = \nu_+ - \nu_- = \frac{c\gamma}{\pi L_{eff}}. \tag{11}$$

This result corresponds to the classical case of a dual frequency laser where the two polarization eigenstates are linear, orthogonal to each other and aligned with the neutral axes of the intracavity birefringent crystal. Moreover, the two eigenfrequencies are not degenerate anymore and their frequency difference is proportional to both the birefringence of the crystal and the Free Spectral Range (FSR) of the laser.

2.1.2 The linear phase anisotropy is zero, $\gamma = 0$

In this case, it is assumed that the linear birefringence is negligible so that the laser cavity has only a circular gain dichroism. The diagonalization of $[J_L]$ leads to:

$$\frac{E_y}{E_x} = \pm i = e^{\pm i\frac{\pi}{2}}. \tag{12}$$

Thus, the eigenpolarizations are right and left handed circular. However, contrary to a cavity that contains a circular anisotropy, the two eigenfrequencies are degenerate. In this particular case the characteristic polynomial is given by $(\lambda - 1)^2 = \Delta G_N^2/4$ whose solutions are $\lambda_\pm = 1 \pm \Delta G_N/2$. Since the two eigenvalues are real, the frequency difference between the two eigenstates (which is proportional to the complex argument) is zero. However, since the complex magnitudes are different, the two laser eigenstates will experience different gains so that:

$$G_\pm = \frac{1}{\sqrt{R}\left(1 \pm \frac{1}{2}\Delta G_N\right)}. \tag{13}$$

Such gain dependence implies a threshold modification of the laser which has been observed experimentally and modelled theoretically [20]. This effect appears naturally in the VSPIN model throughout the modulus of the two possible eigenvalues. As a result, when the laser turns on, the eigenstate experiencing the highest gain (right handed circular if $\Delta G_N > 0$) will oscillate first. When the pump power is increased, the second eigenstate (left handed circular if $\Delta G_N > 0$) will start oscillating provided that the nonlinear coupling constant C between the two modes is lower than 1 (see last section). Moreover, if the self-saturation and cross-

Optics EXPRESS

saturation coefficients coupling the field to the active medium are identical for both eigenmodes, the two eigenmodes are expected to exhibit roughly the same intensities far above threshold. The two eigenstates are degenerate in frequency so the laser polarization emitted will evolve from circularly-polarized close to threshold to linearly-polarized very far above threshold. Consequently, the circular polarization rate is expected to sharply decrease as soon as the second eigenpolarization starts oscillating. This mechanism describes quite accurately the observations reported by Iba et al. with monolithic (110) VCSELs in [29].

2.1.3 General case: $\Delta G \neq 0$ and $\gamma \neq 0$ (some effective spin-polarization in the active medium and non-ideal cold cavity)

In order to simplify the problem, we assume in the following that ΔG and γ are both positive values. Accounting for this condition and according to the characteristic polynomial of Eq. (8), three cases must now be considered.

2.1.3.1 The phase anisotropy is dominant $\Delta G_N^2 < 4\sin^2(\gamma)$ (linear birefringence overpowers the effective spin injection in the active medium)

In this case, the eigenvalues $\lambda_\pm$ have complex values:

$$\lambda_\pm = \cos(\gamma) \pm i\sqrt{\sin^2(\gamma) - \frac{1}{4}\Delta G_N^2}. \tag{14}$$

The imaginary part of the eigenvalues lifts the frequency degeneracy so that each eigenstate now has its own oscillation frequency. By developing Eq. (8), one finds that the frequency difference reads

$$\Delta\nu = \nu_+ - \nu_- = \frac{c}{\pi L_{eff}} \arctan\left(\tan(\gamma)\sqrt{1-\left(\frac{\Delta G_N}{2\sin(\gamma)}\right)^2}\right). \tag{15}$$

The evolution of the frequency difference as a function of r is plotted in Fig. 2, where r refers to the ratio $\Delta G_N / 2\sin(\gamma)$.

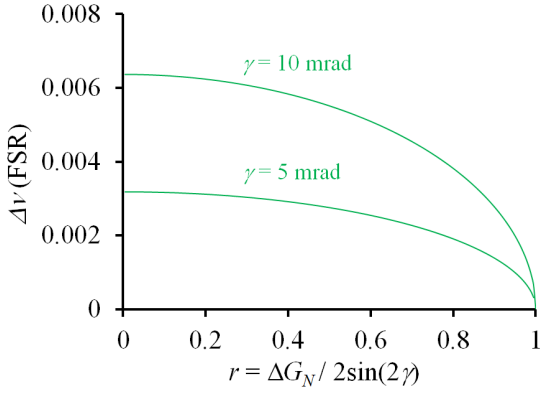

Fig. 2. Evolution of the frequency splitting between the two polarization eigenstates as a function of the ratio r between the circular dichroism of gain ΔG_N and the linear birefringence of phase γ.

For a given phase anisotropy, the frequency difference decreases as the gain circular dichroism increases. More precisely, $\Delta\nu$ remains almost constant for low to moderate values

Optics EXPRESS

of ΔG_N, i.e. $\Delta G_N < \sin(\gamma)/10$, and drops abruptly when ΔG_N approaches $2\sin(\gamma)$. This behavior leads to frequency locking when $\Delta G_N = 2\sin(\gamma)$, which translates to $r = 1$.

We now investigate how the laser polarization state evolves with respect to the gain circular dichroism ΔG_N. The two allowed polarization states correspond to the eigenvectors of the laser Jones matrix $[J_L]$. Taking into account the eigenvalue expression of Eq. (14), the x and y components of the electric field satisfy the relation

$$\frac{E_y}{E_x} = -\frac{2\sin(\gamma)}{\Delta G_N}\left(1 \pm \sqrt{1-\left(\frac{\Delta G_N}{2\sin(\gamma)}\right)^2}\right). \tag{16}$$

Introducing r, the previous expression simplifies to

$$\frac{E_y}{E_x} = -\frac{1}{r}\left(1 \pm \sqrt{1-r^2}\right). \tag{17}$$

The two eigenstates are thus two linear polarizations whose orientations depend on the ratio between the gain circular dichroism and the linear birefringence (see Fig. 3). Consequently, if both modes are emitting the polarization of the total light field is time-dependent due to the time-dependent phase difference. The polarization rotates around the Poincaré sphere at a rate corresponding to the frequency difference [31]. This behavior is observed by Gerhardt et al. [32] and described as an ultrafast spin-induced polarization oscillation. It is worth highlighting that the presence of gain circular dichroism breaks the orthogonality between the two polarizations. For a fixed linear birefringence, as ΔG_N increases, the two polarizations progressively align along a common direction at ± 45° with respect to the crossed initial orientations until they become perfectly aligned for r = 1. In this unique situation the two eigenstates become degenerate in terms of polarization and frequency.

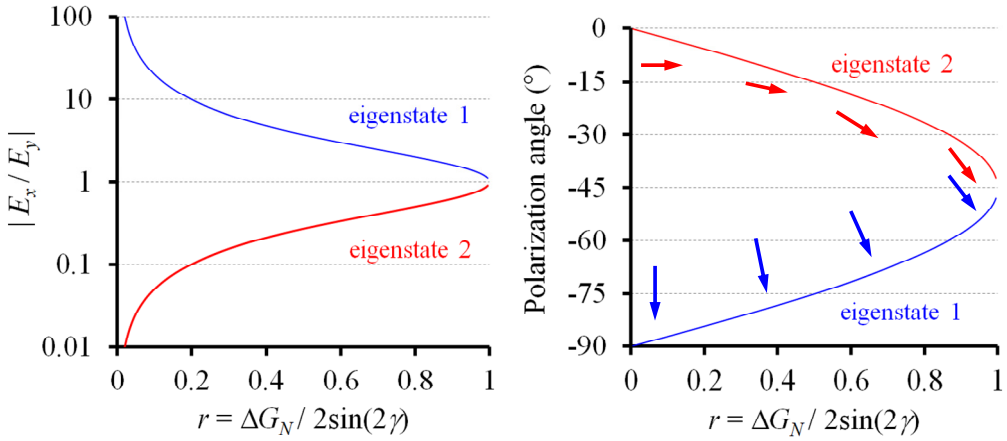

Fig. 3. Ratio of the transverse components of the filed (left-hand side) and polarization angle (right-hand side) for the two possible eigenstates as a function of the ratio r between the circular dichroism of gain and the linear birefringence of phase.

Optics EXPRESS

2.1.3.2 Balanced phase anisotropy and gain circular dichroism $\Delta G_N^2 = 4\sin^2(\gamma)$ (Effective spin-polarization in the active medium compensates the linear phase anisotropy of the cold cavity)

This is the unique situation mentioned above. In this case the characteristic polynomial of Eq. (8) has a single solution $\lambda_\pm = \cos(\gamma)$ and the electromagnetic field satisfies $E_y/E_x = -1$. The eigenstates are two indistinguishable linear polarizations that are collinear with degenerate frequencies. Consequently, the laser beam consists of one polarization oriented at –45° with respect to the neutral birefringence. Hence, the continuity between cases 2.1.3.1 and 2.1.3.2 is well verified.

2.1.3.3 The gain circular dichroism is dominant $\Delta G_N^2 > 4\sin^2(\gamma)$ (Effective spin-polarization in the active medium overpowers the linear phase anisotropy of the cold cavity)

In this case, the characteristic polynomial has two solutions which are both real

$$\lambda_\pm = \cos(\gamma) \pm \sqrt{\frac{1}{4}\Delta G_N^2 - \sin^2(\gamma)}. \tag{18}$$

Consequently, the two eigenpolarizations exhibit degenerate frequencies. In practice, the laser output polarization is unique and results from the linear superposition of the two eigenstates. The output polarization state evolves as a function of the pump rate and the amount of gain dichroism since the possible oscillation of the eigenstates is directly controlled by the gain dichroism itself (oscillation condition). The x and y components of the electrical field satisfy the relation:

$$\frac{E_y}{E_x} = -2\frac{e^{-i\gamma} - \lambda_\pm}{i\Delta G_N}, \tag{19}$$

whose resolution in polar coordinate gives for the module

$$\left|\frac{E_y}{E_x}\right| = 1, \tag{20}$$

and for the phase

$$\Phi_\pm = \arg\left(\frac{E_y}{E_x}\right) = \mp \arctan\left(r^2 - 1\right)^{-\frac{1}{2}}. \tag{21}$$

Thus the two possible eigenstates exhibit elliptical polarization, as shown in Fig. 4.

Optics EXPRESS

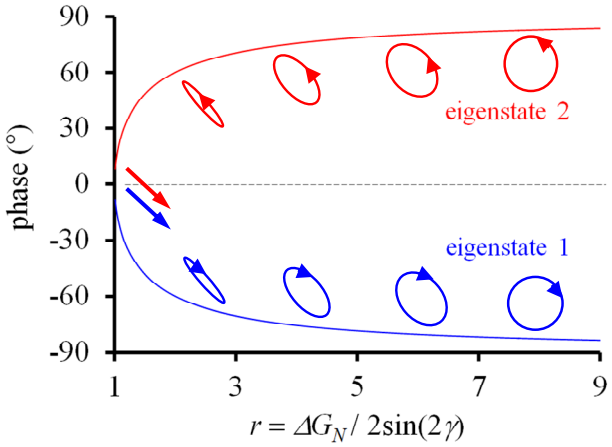

Fig. 4. Evolution of the two eigenpolarizations as a function of the ratio r between the circular dichroism of gain ΔG_N and the linear birefringence of phase γ.

When the gain circular dichroism is very large compared the phase anisotropy (which also implies that the phase anisotropy is negligible), the two eigenstates lead to a single perfectly circularly-polarized state as $\lim_{\gamma\to 0}\Phi_{\pm} = \pm\pi/2$. At the same time, the continuity condition between the case 2.1.3.2 and 2.1.3.3 is fulfilled. Besides, the characteristic polynomial provides the gain seen by each eigenstate:

$$G_{\pm} = \sqrt[-1]{R}\left(\cos(\gamma) \pm \sin(\gamma)\sqrt{r^2-1}\right)^{-1}. \tag{22}$$

In practice, the eigenstate experiencing the highest gain prevails. In our case, the eigenstate labeled 1 in Fig. 4 will preferentially oscillate. As previously mentioned, if the nonlinear coupling constant C between the two eigenstates is lower than 1, the eigenstate labeled 2 will reach the oscillating regime for a pumping rate superior to that of eigenstate 1. The appearance of this second eigenstate will lead to a diminution of the circular polarization degree. If C >1, then only the first eigenstate oscillates and the simultaneous oscillation of both eigenstates in the cavity is impossible for any given pumping power. In this case, the circular polarization degree increases indefinitely with the pumping power. In other words, since the eigenfrequencies are degenerate, the output beam of the laser exhibits a unique polarization state formed by the linear superposition of the two possible eigenpolarizations.

2.1.4 Summary

Figure 5 summarizes the previous results regarding the vectorial behavior of a laser with circular dichroism of gain in the active medium and residual linear birefringence in the cavity. Regardless of its magnitude, the linear birefringence is always present in a laser due to residual constraints in the active medium or/and in the optical components inside the laser cavity. In this framework, the model shows that when there is no gain circular dichroism in the active medium the laser eigenstates correspond to two orthogonal linear polarizations with a frequency difference proportional to the linear birefringence. As the gain circular dichroism increases, the two eigenstates lose their orthogonality and the two linear polarizations progressively rotate and align along a common direction while the eigenfrequencies remain almost constant. When the gain circular dichroism is sufficiently high, the two linear polarizations become superposed and the associated eigenstates become degenerate due to phase locking. In this unique situation the laser emits a single polarization oriented at 45° with respect to the neutral axes of the linear birefringence.

Optics EXPRESS

When the gain circular dichroism increases further, the polarization states evolve from linear to elliptical with the long axis oriented at 45°. This ellipticity degree decreases as the gain circular dichroism keeps increasing until the polarization states become circular. Note that, in the region where the polarization states are elliptical, the eigenstate 2 with an elliptical polarization orthogonal to the eigenstate 1 can oscillate if the nonlinear coupling constant C (ruled by the cross gain saturation) is lower than 1. If $C < 1$, the eigenstate experiencing the less gain will start oscillating after the dominant eigenstate when the pump power is increased. Consequently a decrease of the degree of circular polarization can be observed when the laser is operated far above threshold as already shown by Iba et al. in a circularly polarized GaAs quantum wells spin injected VCSEL [29].

By considering the theoretical predictions above, circular polarization can be obtained only if the ratio r between the circular gain dichroism and the linear phase birefringence is much higher than one. In VCSEL structures, the effective circular gain dichroism induced by spin injection being extremely low, the linear phase birefringence has to be reduced so that the effect of spin injection on the laser polarization is revealed. Based on this conclusion, we have undertaken to compensate the residual linear phase birefringence in an extended cavity VCSEL using an intracavity voltage controlled PLZT (Lead Lanthanum Zirconium Titanate) electro optical ceramic [23]. We then succeeded to decrease the cavity birefringence from 21 mrad to less than 0.5 mrad, corresponding to a 40 fold reduction. By changing the pump polarization from left (σ -) to right (σ +) -handed circular, we observed a rotation of 4° of the laser output polarization [23]. Even weak, this effect was not observable before reducing the linear birefringence.

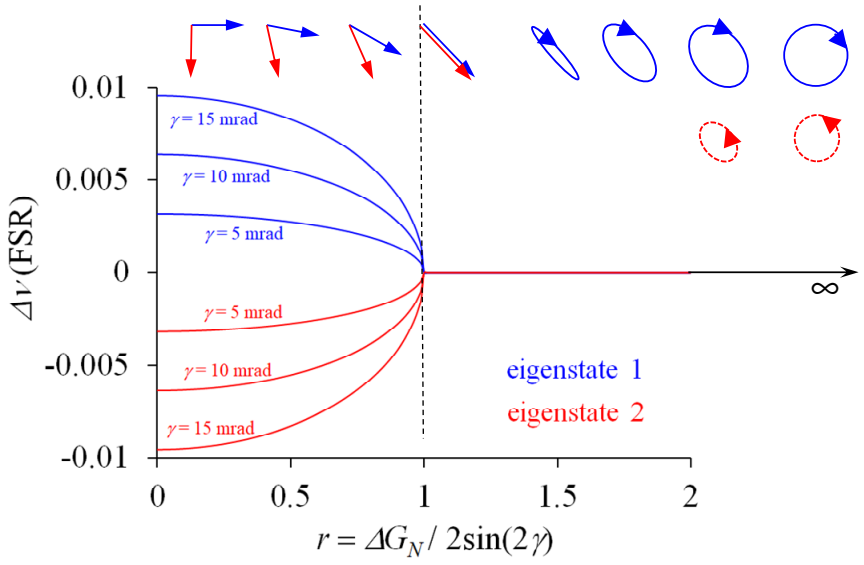

Fig. 5. Evolution of the frequency splitting and the two eigenpolarizations as a function of the ratio r between the circular dichroism of gain ΔG_N and the linear birefringence of phase γ.

3. Towards a laser cavity optimized for polarization switching by spin injection

The previous section highlighted that a residual linear birefringence in the laser forces the oscillation of crossed linearly polarized eigenstates. Thus, the laser naturally oscillates with respect to one of these eigenstates or possibly both if the coupling constant in the active medium is low enough. In practice, spin injection is expected to generate a weak circular gain dichroism ΔG_N due to spin decoherence, which will break the orthogonality between the two linearly polarized eigenstates. Additionally, the nonlinear coupling constant being high in semiconductor active media [33], the laser output polarization is expected to be linearly

Optics EXPRESS

polarized with an orientation affected by the spin injection. Consequently, triggering a polarization switch from a given polarization state to the orthogonal polarization state by leveraging moderately effective spin injection (low effective circular gain dichroism) will only be possible if the laser cavity has been "prepared" to inherently sustain oscillations of circularly polarized eigenstates. This configuration can be achieved by inserting a non-reciprocal element such as a Faraday rotator inside the laser cavity [34]. This section addresses the modeling of such a laser cavity illustrated in Fig. 6.

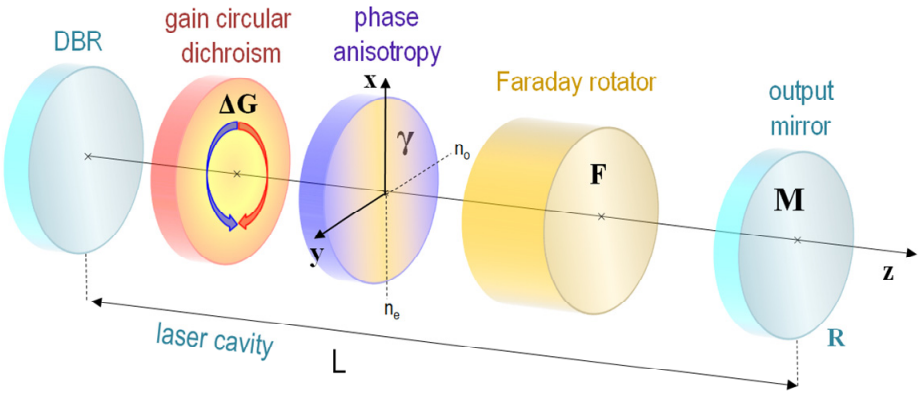

Fig. 6. Schematic representation of the cavity including a Faraday rotator.

3.1 Jones formalism

The Jones matrix associated to the Faraday rotator reads:

$$[J_F] = \sqrt{R}\begin{bmatrix} \cos\theta & -\sin\theta \\ \sin\theta & \cos\theta \end{bmatrix}, \tag{23}$$

where θ is the rotation angle of a linearly polarized field crossing the Faraday rotator. This angle is proportional to the Verdet constant, the thickness of the component and the applied magnetic field. The eigenstates of such a matrix are two circular polarizations, right-handed and left-handed irrespective to the value of θ . In practice, θ is adjusted to $\pi/4$ in optical isolators such that a linear polarization crossing the element back and forth experiences a rotation of $\pi/2$. In the case considered here, θ is chosen to be $\pi/4$ to ensure that the circular birefringence induced by the Faraday rotator dominates any residual linear birefringence in the laser. In this case, the Jones matrix associated with the Faraday rotator simplifies to:

$$[J_F] = \frac{1}{\sqrt{2}}\begin{bmatrix} 1 & -1 \\ 1 & 1 \end{bmatrix}. \tag{24}$$

It is important to note that this operator couples the linear polarizations. Accounting for the Faraday rotator, the total Jones matrix of the field at the output mirror for one round trip in the cavity becomes:

$$[J_L] = e^{i\phi}[J_F][J_{\Delta\phi}][J_G][J_{\Delta\phi}][J_F][J_M]. \tag{25}$$

$[J_{\Delta\Phi}]$ is the Jones matrix of the residual linear birefringence in the active medium given by Eq. (1). $[J_G]$ is the Jones matrix of the circular gain dichroism induced by spin injection in the active medium given by Eq. (3). Finally, $[J_M]$ is the Jones matrix of the mirror given by Eq. (4). In the following, we keep the same notations as in the previous section. The

Optics EXPRESS

normalized gain circular dichroism ΔG_N accounts for one round trip in the active medium while $e^{j\phi}$ represents the cumulative phase rotation of the electromagnetic field after one round trip propagation through the laser cavity. The cumulative phase now accounts for the optical path in the Faraday rotator, so that:

$$\phi = 2k\,(\,n_{ma}e_{ma} + \overline{n}l + n_F e_F + L\,) = 2k\,L_{eff}\,, \tag{26}$$

where, n_F and e_F are the mean optical index and the thickness of the Faraday rotator respectively. With this new Jones matrix, the resonance condition of the field $\vec{E}$ for one round trip in the cavity must satisfy $[J_L]\vec{E} = \lambda\vec{E}$. The diagonalization of this Jones matrix leads to two new polarization eigenstates with their associated eigenvalues. In the special case where $\theta = \pi/4$, the equations greatly simplify leading to the following characteristic polynomial

$$\lambda_{\pm} = e^{i\frac{\pi}{2}}\left(\mp 2 - \Delta G_N\right). \tag{27}$$

As anticipated, the residual phase anisotropy that might exist in the laser or the active medium itself does not play any role in the characteristic polynomial. To highlight a physical insight, one can rewrite the latest equation as follows:

$$\lambda_{\pm} = \left(\,2 \pm \Delta G_N\right) e^{\mp i\frac{\pi}{2}}. \tag{28}$$

The modulus of this expression gives the gain seen by each polarization eigenstate, that is

$$G_{\pm} = \frac{1}{\sqrt{R}}\left(1 \pm \frac{1}{2}\Delta G_N\right)^{-1}, \tag{29}$$

whereas, its argument provides the two eigenfrequencies of the laser,

$$\nu_{\pm} = \left(q \mp \frac{1}{4}\right)\frac{c}{L_{eff}}, \tag{30}$$

where q is an integer. Thus, the frequency difference between the two eigenstates is:

$$\Delta\nu_{\pm} = \left|\nu_{+} - \nu_{-}\right| = \frac{c}{4L_{eff}}. \tag{31}$$

Note that the frequency difference is independent of the linear phase anisotropy in the active medium. The frequency shift is only imposed by the Faraday rotator and is precisely equal to half the free spectral range of the laser. Furthermore, the two eigenstates of the laser can be obtained by diagonalization of the Jones matrix. It can be shown in a straightforward way that the transverse components of the field along x and y satisfy the expression

$$\left.\frac{E_x}{E_y}\right|_{\pm} = -i\tan(\gamma) \pm i\sqrt{\tan^2(\gamma) + 1}, \tag{32}$$

which proves that the two transverse components of the field are always in quadrature for each of the two laser eigenstates. Furthermore, the gain circular dichroism ΔG_N is not present in this expression, so the circular dichroism induced by the electronic spin will have no influence on the laser eigenpolarizations. However, as shown by Eq. (29), the circular dichroism will favor the oscillation of one eigenstate. The question of simultaneity and efficiency of the polarization switching with respect to the coupling constant C will be addressed in the final section.

Optics EXPRESS

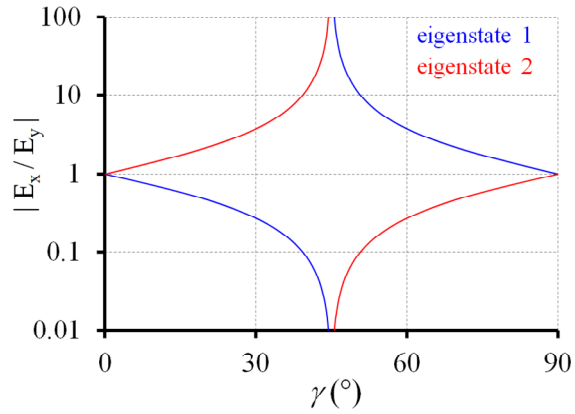

Fig. 7. Ratio of the transverse components of the two eigenstates with respect to the linear birefringence in the active medium.

The evolution of the transverse components of the field with respect to the linear birefringence is reported on a logarithmic scale in Fig. 7. Note the existence of a singularity for $\gamma = 45°$. Although the case is anecdotal since the linear birefringence under consideration is supposed to be residual, it is further detailed along with other specific cases for completeness.

3.2 Study of specific cases

3.2.1 Case where the linear phase anisotropy is zero, $\gamma = 0$

When the linear anisotropy of phase is null,

$$\left.\frac{E_x}{E_y}\right|_{\pm} = \pm i. \tag{33}$$

The two eigenpolarizations of the laser are respectively right- and left-circularly polarized.

3.2.2 Case where the phase anisotropy is equal to 90°

A Taylor expansion of Eq. (32) around $\gamma = 90°$ leads to the two eigenstates

$$\left.\lim_{\gamma \to \frac{\pi}{2}} \frac{E_x}{E_y}\right|_{+} = -\infty \tag{34}$$

and

$$\left.\lim_{\gamma \to \frac{\pi}{2}} \frac{E_x}{E_y}\right|_{-} = 0. \tag{35}$$

In this unique case, the two possible polarizations are linear and oriented along the x and y axes respectively, i.e., along the neutral axes of the phase anisotropy.

3.2.3 General case

When the residual birefringence is neither null nor 90°, the two laser eigenstates are almost perfectly left and right circularly-polarized (see Fig. 8-left). They evolve to elliptical polarization in the vicinity of $\gamma = 90°$, and further to linear polarization at $\gamma = 90°$. In practice, because the linear birefringence is a residual birefringence, it is reasonable to assume that the

Optics EXPRESS

insertion of a Faraday rotator into the laser leads to two possible circularly-polarized eigenpolarizations. Moreover, as shown in Fig. 8-right, the frequency difference between these two eigenstates remains constant and equals half the free spectral range of the laser cavity independent of the linear birefringence value.

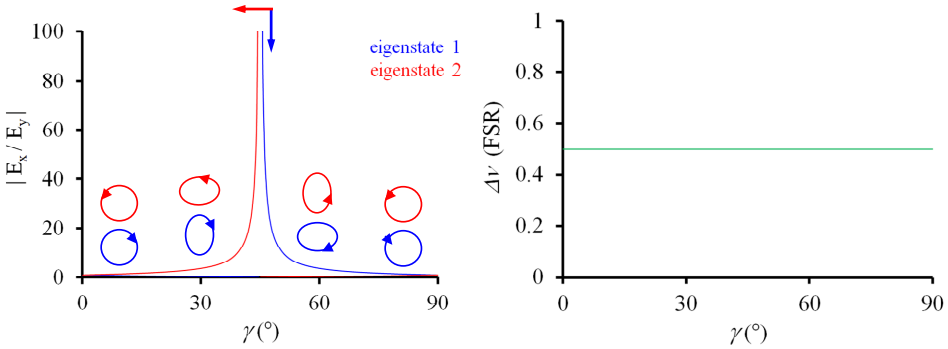

Fig. 8. (left) Evolution of the ellipticity and (right) Frequency difference between the two laser eigenstates as a function of the linear birefringence in the active medium.

3.2.4 Summary

The insertion of a Faraday rotator in the VECSEL cavity enables the preparation of the laser in the optimal configuration for observing full polarization switching under low effective spin injection. Moreover, such a rotator offers a good way to overcome the detrimental contributions of any residual linear birefringence in the active medium and/or cold cavity providing natural oscillations of the right- or left- handed circular polarizations. Within this framework, the circular gain dichroism ΔG_N induced by the spin injection unbalances the gain experienced by each eigenstate leading to the possibility of a full polarization switch provided that the nonlinear coupling constant C between the two eigenstates is high enough (which is the case in semiconductor active media [33]). In addition, the vectorial VSPIN model shows that the frequency difference between the two eigenstates is equal to half the laser free spectral range regardless the value of the linear birefringence in the laser. The impact of the nonlinear coupling constant on the polarization switching efficiency is considered in the following section.

4. Role of nonlinear coupling strength with respect to the gain dichroism on the polarization switching effectiveness

We showed in the previous section that the laser cavity can be prepared so that a tiny gain circular dichroism induced by spin injection can induce a complete polarization switch. In practice, a laser cavity incorporating a non-reciprocal effect such as a Faraday rotator offers a simple way to achieve this polarization switching by concealing the effect of residual linear birefringence in the laser. Hence, the gain circular dichroism induced by spin injection effectively acts as an imbalance of gain between the two circularly polarized eigenstates favoring the oscillation of one eigenstate with respect to the other. This gain imbalance, even low, can trigger a fast and complete [35] polarization switch provided that the nonlinear coupling constant between the eigenstates is high enough to achieve the required leverage effect.

In a Class-A laser, the population inversion densities can be adiabatically eliminated. Under this condition, the laser behavior is described by two first order coupled differential equations which rule the temporal evolution of the two intensities. We define I_R and I_L as the right- and left-circular polarization intensities respectively, α_R and α_L the non-saturated gains of the right- and left-circular polarizations, β_R and β_L the self-saturation coefficients of the right- and left-circular polarizations, θ_{RL} the cross-saturation coefficient of the right-circular

Optics EXPRESS

polarization by the left-circular polarization, and θ_{LR} the cross-saturation coefficient of the left-circular polarization by the right-circular polarization. With these notations, the two coupled equations read:

$$\dot{I}_R = \alpha_R - \beta_R I_R - \theta_{RL} I_L, \tag{36}$$

$$\dot{I}_L = \alpha_L - \beta_L I_L - \theta_{LR} I_R. \tag{37}$$

We now assume in first approximation that the two self-saturation coefficients, β_R and β_L, and the two crossed saturation coefficients, θ_{RL} and θ_{LR}, are equal. Furthermore, we assume that the non-saturated gains differ due to the circular dichroism induced by spin injection. The previous notations simplify to

$$\beta_R = \beta_L = \beta, \tag{38}$$

$$\theta_{RL} = \theta_{LR} = \theta, \tag{39}$$

$$\alpha_R = \alpha + \delta\alpha/2, \tag{40}$$

$$\alpha_L = \alpha - \delta\alpha/2. \tag{41}$$

In the steady state, $\dot{I}_R = 0$ and $\dot{I}_L = 0$. Therefore Eq. (36) and Eq. (37) give the intensities of the two modes. Three cases can be distinguished:

4.1 The two eigenstates oscillate: $I_R \neq 0$ and $I_L \neq 0$

$$I_R = \frac{\alpha(\beta-\theta) + \frac{\delta\alpha}{2}(\beta+\theta)}{\beta^2 - \theta^2}, \tag{42}$$

$$I_L = \frac{\alpha(\beta-\theta) - \frac{\delta\alpha}{2}(\beta+\theta)}{\beta^2 - \theta^2}. \tag{43}$$

By introducing the nonlinear coupling constant as defined by Lamb [36],

$$C = \frac{\theta_{RL}\theta_{LR}}{\beta_R\beta_L} \equiv \frac{\theta^2}{\beta^2}. \tag{44}$$

The intensities of the two eigenstates become:

$$I_R = \frac{\alpha}{\beta}\frac{\left(1-\sqrt{C}\right) + \frac{\delta\alpha}{2\alpha}\left(1+\sqrt{C}\right)}{1-C}, \tag{45}$$

$$I_L = \frac{\alpha}{\beta}\frac{\left(1-\sqrt{C}\right) - \frac{\delta\alpha}{2\alpha}\left(1+\sqrt{C}\right)}{1-C}. \tag{46}$$

The value of the coupling constant C depends on a large number of parameters: the nature of the active medium, the orientation of its crystallographic axis, the pumping scheme, and the polarization of the two oscillating modes under consideration [33,37–39]. Nevertheless, this coupling constant can be determined experimentally quite precisely [37] and then inserted into the model. The simultaneous oscillation of the two modes is possible only if C < 1. In our case, we already know that the coupling constant is close but inferior to 1 since simultaneous

Optics EXPRESS

oscillations of the eigenstates were experimentally observed [40]. Equation (45) and Eq. (46) show that the two intensities behave antagonistically as the gain circular dichroism $\delta\alpha$ increases, and that their evolution accelerates when the nonlinear coupling constant converges toward 1.

4.2 The right circular polarization only oscillate: $I_R \neq 0$ and $I_L = 0$

Once the intensity of left-circular polarization I_L reaches zero due to the gain unbalance, I_R follows a new expression given by:

$$I_R = \frac{\alpha}{\beta}\left(1+\frac{\delta\alpha}{2\alpha}\right), \tag{47}$$

where $I_L = 0$. The intensity of the right-circular polarization eigenstate increases linearly with respect to $\delta\alpha$ and does not depend on the coupling constant anymore.

4.3 The left circular polarization only oscillates: $I_R = 0$ and $I_L \neq 0$

In this case, the intensity of left-circular polarization I_L becomes

$$I_L = \frac{\alpha}{\beta}\left(1-\frac{\delta\alpha}{2\alpha}\right), \tag{48}$$

where $I_R = 0$. Similarly, the intensity of the left-circular polarization eigenstate decreases linearly with respect to $\delta\alpha$ and does not depend on the coupling constant anymore.

4.4 Discussion

The simultaneous oscillation of the two eigenstates is possible only if the nonlinear coupling constant between these two eigenstates is inferior to 1, which is the case in VECSELs. The graphs in Fig. 9 illustrate how the intensities of the two eigenstates evolve with respect to the normalized gain circular dichroism for three values of the coupling constant: $C = 0$, $C = 0.5$, and $C = 0.9$. When the coupling constant is zero, the intensities of the two eigenstates move independently and are proportional to the normalized gain circular dichroism. When the coupling constant is non zero, a region where the two eigenstates are allowed to oscillate simultaneously appears (see Fig. 9 for $C = 0.5$). When the coupling constant approaches 1, the simultaneity region narrows down favoring switching from one eigenstate to the other, i.e., from one polarization state to the other.

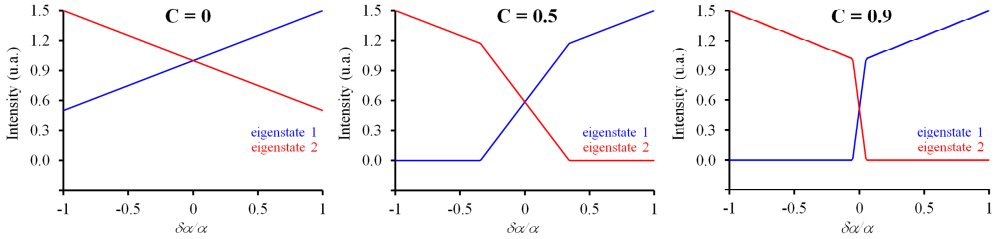

Fig. 9. Evolution of the intensities of the two modes as a function of the normalized circular dichroism of gain for three values of the nonlinear coupling constant: 0, 0.5 and 0.9.

For example, in the case of $C = 0.9$, a gain dichroism as low as 10% is expected to enable a full switch of the laser polarization. The average gain of the active medium being of few percent in VECSELs and the coupling constant being approximatively 0.9, a gain circular dichroism less than 1/1000 should be sufficient to flip the laser polarization. The existence of a coupling constant in a laser acts as a lever to enhance the effectiveness of spin induced gain dichroism to trigger a polarization switching of the laser. In addition to this leverage effect, it

Optics EXPRESS

must be reminded that the laser sustains the oscillation of two eigenstates whose polarizations are perfectly defined. This make the development of circularly polarized spin controlled VECSEL very attractive in terms of polarization purity as compared to Spin-LEDs. The VSPIN model thus predicts that, although the effective spin injection is low and a residual linear birefringence is present, the laser cavity can be prepared so that a full polarization switch from σ^+ to σ^- occurs. We have validated this prediction experimentally using a M-shaped VECSEL cavity including a Faraday rotator [22]. By changing the pump polarization from right to left circular polarization, we observed a corresponding switch from σ^+ to σ^- of the laser polarization. We also observed a threshold reduction of few percent when pumping circularly compare to the linearly polarized pumping. More importantly, the range of simultaneous oscillations of the two eigenstates is shown experimentally to be very narrow favoring then an easy switch from one eigenstate to the other even if ΔG is very low. As shown in Fig. 9, for $C = 0.9$, a normalized gain dichroism of about 10% is sufficient to tip over the polarization. The average gain of the structure being around 1%, a gain dichroism of about 0.1% was shown to be sufficient to fully switch the laser polarization thanks to the leverage effect of the non-linear mode coupling.

5. Conclusion

In this paper, we present a step-by-step derivation of the vectorial model we used to guide our research on the development and optimization of VCSEL based spin lasers [22,23]. This model relies on the Jones formalism where the spin injection effect is phenomenologically taken into account as a gain circular dichroism. The primary focus of this vectorial model is the steady-state operation of the laser. Outside this region which is limited by the longest time constant of the system, i.e., the carrier recombination lifetime or the photon lifetime in the cavity or the spin relaxation lifetime, the dynamical interaction of the electromagnetic field with the active medium has to be taken into account. We show that the resonance condition for the field in the laser cavity yields two possible eigenpolarizations whose coexistence is ruled by the nonlinear coupling constant as defined by Lamb. The gain circular dichroism is intentionally considered low due to the unavoidable spin relaxation in semiconductor quantum wells. Under this condition, we show that the residual linear birefringence that is inherently present in any laser forbids the polarization to switch from one state to the other. The laser polarization is then mainly ruled by this linear birefringence, which forces the laser to operate in two possible linear polarizations oriented along the neutral axes of the birefringence. Increasing spin injection breaks the orthogonality between the two possible polarizations, which progressively align along a common direction oriented at 45° while staying linear. Increasing the spin injection further might lead to a peculiar situation, where the two possible polarizations are degenerated and correspond to a single linear polarization oriented at 45° with respect to the neutral axes of the linear birefringence. Above this point, i.e., for very efficient spin injection, the two permitted laser polarizations become elliptical and then circular with opposite directions. In this framework, if the coupling constant is high, one polarization will be dominant. The laser provides a linear polarization whose orientation changes with increasing spin injection until it reaches 45°. At this point the laser polarization becomes elliptical and its ellipticity decreases for strong spin injection. By contrast, if the coupling constant is low, the two possible polarizations oscillate simultaneously. The laser exhibits two distinct crossed linear polarizations which mutually move towards the same direction at 45° till becoming degenerate. Above this point, the two oscillating polarizations become elliptical. Given the fact that they are elliptical with opposite directions and that their frequency is degenerated, the combined output polarization remains linear and oriented at 45°, meaning that the laser outputs always a linear polarization.

To overcome this problem, which is due to the inherent presence of linear birefringence, we show that the laser has to be prepared so that its two polarization eigenstates are right-handed and left-handed, respectively. This is obtained by inserting a nonreciprocal effect

Optics EXPRESS

within the laser cavity. The vectorial modelling shows that in this case a spin injection effect, even very low, can flip the laser polarization from one state to the other. The residual linear birefringence no longer determines the laser polarization eigenstates, but only introduces a slight change of ellipticity. The two possible polarizations being almost circular, spin injection directly acts on the differential gain between these polarizations unlike the previous case where this differential gain was acting on the two eigenpolarizations at the same time. If the coupling constant is high, the oscillating mode is the one experiencing the highest gain. As a result, a small differential gain is now able to selectively favor either the left-handed or right-handed circular polarization.

Some of these predictions have already been exploited experimentally in [22] and [23] in order to enhance the effect of spin injection on polarization switching. Moreover, this new VSPIN model can also explain several observations such as: threshold reduction [20], time dependent polarization oscillation [32], possible decrease of the circular polarization degree far above threshold [29], and the evolution of the polarization orientation according to the residual birefringence in the laser [23]. The insertion of a nonreciprocal effect in the laser cavity is predicted and proved to be a very efficient way to hide the residual linear birefringence and thus to obtain a full polarization flip by spin injection in VECSELs [22]. However, the integration of a nonreciprocal component in a commercial product is projected to be challenging. From a practical viewpoint, compensating the residual linear birefringence is an alternative solution that should be more affordable for integration. Indeed, the vectorial model presented here shows that the gain circular dichroism generated by spin injection must be much larger than the linear birefringence. Combined with the leverage effect provided by the high coupling constant in VCESELs, an almost full polarization switch might be obtained for inefficient spin injection provided that the linear birefringence is cancelled. This is the approach that we are currently exploring.

Funding

French National Research Agency, project INSPIRE.

Acknowledgment

The authors acknowledge Henri Jaffrès for fruitful discussions on spin dynamics in solid-state devices.